Supporting Online Material for

Graphene Visualizes the First Water Adlayers on Mica at Ambient Conditions

Ke Xu, Peigen Cao, James R. Heath*

*To whom correspondence should be addressed. E-mail: heath@caltech.edu

Published 3 September 2010, *Science* **329**, 1188 (2010)
DOI: 10.1126/science.1192907

This PDF file includes:

Supporting Online Material

Materials and Methods

Sample preparation. Single and few-layer graphene sheets were prepared by the standard method of mechanical exfoliation (Novoselov *et al.* 2005; Lui *et al.* 2009) of Kish graphite on freshly cleaved muscovite mica (Grade V1; round disks of diameter 10 mm, Ted Pella). All experiments were performed at room temperature (22±2 °C). Humidity was monitored using a Fluke 971 temperature humidity meter. For graphene deposited on mica at ambient conditions, the ambient relative humidity (RH) was measured to be in a range of 36% to 42%. The low humidity experiment was carried out in a glove-bag (Sigma-Aldrich AtmosBag) that was purged and protected under a continuous flow of ultra-high purity argon. Mica disks were first heated in air at 200 °C for 10 min to remove any absorbed moisture, and then transferred into the glove-bag. The mica surface was cleaved in the glove-bag and allowed to equilibrate for ~5 min before graphene was deposited. A reading of RH = 1.8% to 2.1% was recorded for the process. The high humidity experiment was carried out in a chamber with a beaker of water at the center. The mica surface was cleaved in the chamber and allowed to equilibrate for ~5 min before graphene was deposited. A reading of RH = 89±2% was recorded during the process.

Identification of graphene layers. Graphene mono- and few-layers were identified through optical microscopy and confirmed by spatially resolved Raman spectroscopy. In the optical search process, we found it was easier to identify the thinnest graphene sheets using transmitted light (Fig. S1). Raman spectra were recorded with a Renishaw M1000 Micro Raman spectrometer system using a 514.5 nm laser beam and a 2400 lines per mm grating. A confocal optical microscope with a ×100 objective lens was used to record spectra with a spatial resolution of 2 μm. No noticeable D peak was observed in the Raman spectra of the deposited graphene (Figs. S1, S2), which is suggestive of high-crystalline order of our samples. The sizes of the identified graphene mono- and few-layers range from tens of micrometers to more than 100 micrometers.

Atomic Force Microscopy. AFM images were obtained on a Digital Instrument Nanoscope IIIA AFM in tapping mode at ambient conditions. A sharp TESP tip (Veeco) was used in the experiment. Typical values for the force constant, resonance frequency and tip radius were 42 N/m, 320 kHz, and 8 nm, respectively. Height calibrations were performed using the step heights of freshly cleaved graphite samples.

Supplementary Figures, with Additional Discussion in the Captions

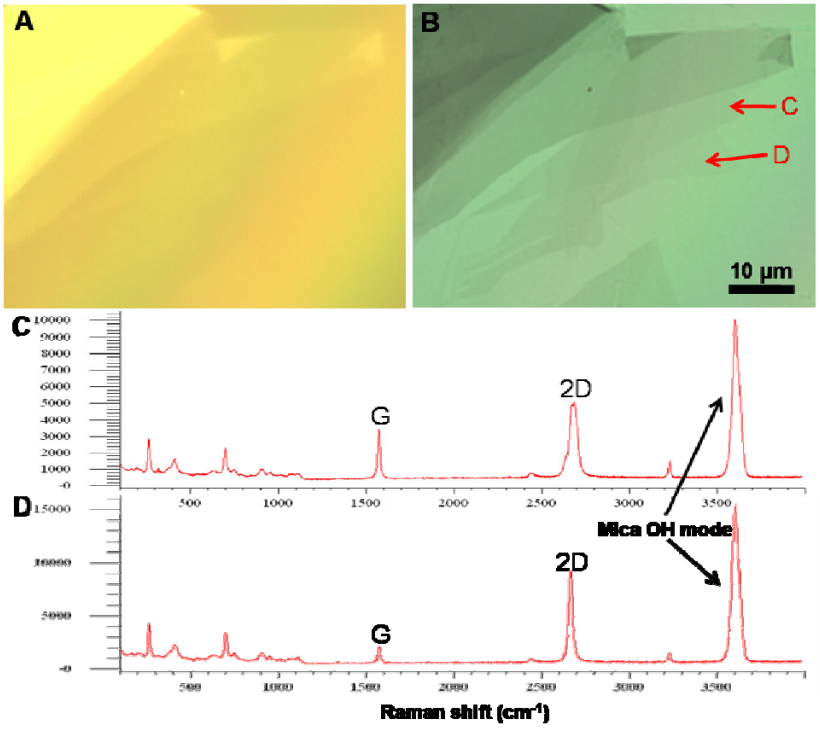

Fig. S1. Few-layer graphene sheets are most readily observed through transmission optical microscopy. (**A**) In reflective optical microscopy, the thinnest graphene sheets are hard to see. (**B**) Transmission optical microscopy of the same area reveals the thinnest graphene sheets. (**C** and **D**) Raman spectra of two different regions of the graphene sheets as indicated in (B), corresponding to bilayer and monolayer graphene, respectively.

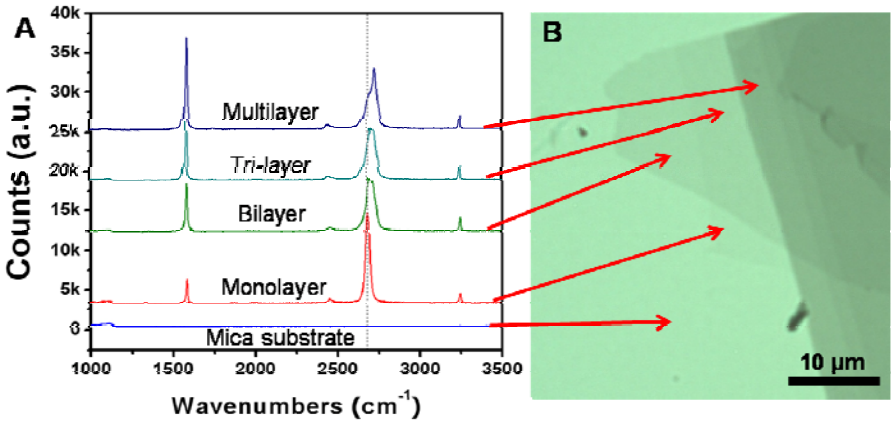

Fig. S2. Identification of numbers of graphene layers in a representative sample. Spatially resolved Raman spectra of different regions in (**B**) are given in (**A**).

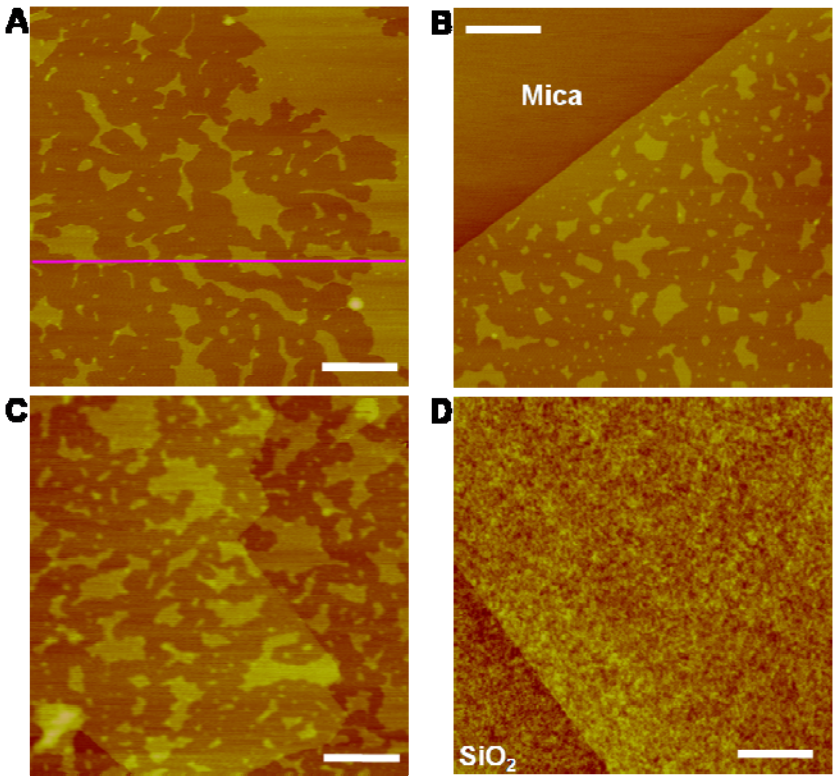

Fig. S3. Additional AFM images of graphene deposited on mica and SiO_2 substrates under ambient conditions. (**A, B**) Additional images of monolayer graphene sheets deposited on mica. Pink line corresponds to the pink height profile in Fig. 1E. (**C**) Image of another graphene-on-mica sample, at the border between bilayer (left) and monolayer (right) graphene sheets. (**D**) Image of a monolayer graphene sheet deposited on SiO_2 at ambient conditions. SiO_2 surfaces have very large surface roughness (standard deviations in height ~0.2 nm), and so adsorbed water molecules cannot form two-dimensional islands. Scale bars: 200 nm for (A) and (C). 500 nm for (B) and (D). The same height scale (4 nm) is used for all images.

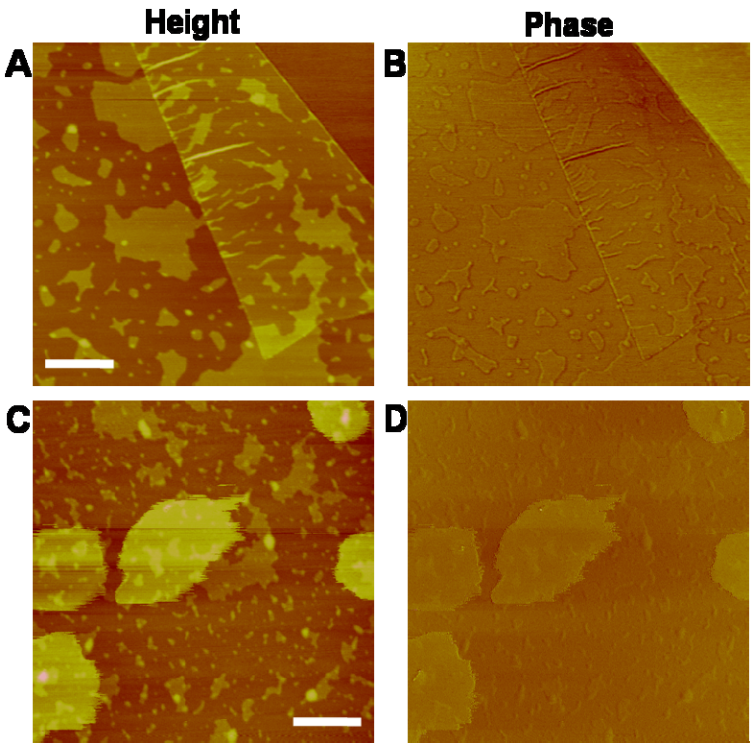

Fig. S4. AFM phase images indicate the island-like plateau structures are under the graphene sheets. (**A**) AFM height image of a monolayer graphene sheet deposited on mica at ambient conditions (Fig. 1F in the main text). The edge of the graphene sheet is folded underneath itself. (**B**) The corresponding phase image. Significant phase difference is observed between the mica (upper right corner) and graphene surfaces, reflecting the difference in surface properties (Garcia and Perez 2002). In contrast, the same phase is observed for the plateaus and other parts of graphene (except for edges, which are always highlighted in phase images), indicating the AFM tip is interacting with the same surface (graphene), and the plateaus are underneath graphene. (**C**) AFM height image of a monolayer graphene sheet deposited on mica at ambient conditions, and then contaminated on the surface by the application of a scotch tape. (**D**) The corresponding phase image of (C). Contrasting phases are observed for the drop-like contaminants on the surface [note how they are dragged along by the tip in (C)]. On the other hand, the same phase is again observed for the plateaus and lower parts of graphene. In agreement with a recent study on friction force microscopy (Lee *et al.* 2010), these results indicate the island-like plateau structures are under the graphene sheets. Scale bars: 200 nm. The same height scale (4 nm) is used for (A) and (C).

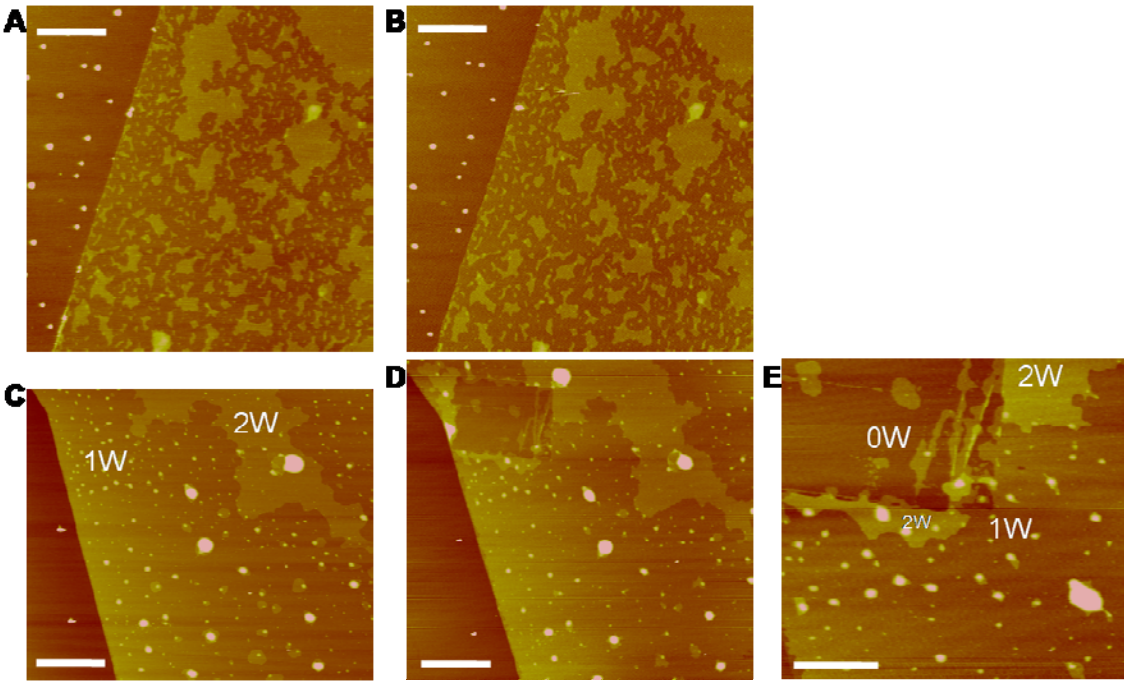

Fig. S5. Stability of the graphene-fixed water patterns. (**A**) Another representative AFM image of a monolayer graphene sheet deposited on mica at ambient conditions. (**B**) The same sample, after being kept at ambient conditions for 25 days. No appreciable change of morphology is observed for the water patterns fixed by graphene. (**C**) An AFM image of monolayer graphene covering both the first (1W) and the second (2W) water adlayers on a mica substrate [from Fig. 3D; realigned with Fig. S5(D)]. (**D**) The same sample, after the entire mica substrate (~0.1 mm thick) was bent upwards by ~15 degrees. This excessive bending caused shear and partial displacement of graphene, and the water adlayer reorganized accordingly (upper left corner of the image). (**E**) A close-up of the change in (D). 0W, 1W, and 2W label the regions where graphene is on top of 0, 1, and 2 adlayers of water, respectively. During bending, water was squeezed out of a square ~1 μm in size and piled up at the edges of the square. Wrinkle-like features attributable to bending were also observed. Such square-like and wrinkle-like features are not observed in any samples that have not been subjected to extensive bending. Scale bars: 500 nm for (A), (B), and (E). 1 μm for (C) and (D). The same height scale (4 nm) is used for all images.

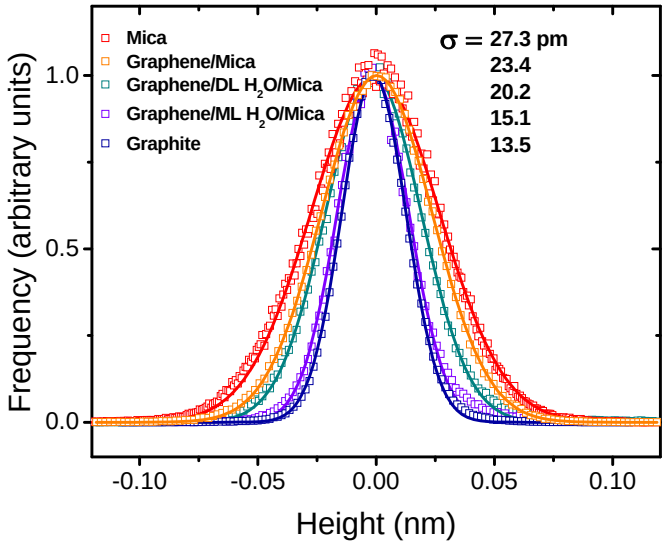

Fig. S6. Comparison of the roughness of different surfaces. Height histograms (open squares) are given for a freshly cleaved mica surface, graphene on bare mica surface (from a sample prepared at 2% RH), graphene on a single water adlayer on mica (labeled as ML H_2O; from a sample prepared at 90% RH), graphene on top of two water adlayers (labeled as DL H_2O; from a sample prepared at 90% RH), and a freshly cleaved graphite surface. The statistics are obtained from scanning over 200×200 nm^2 regions, similar to the conditions used in a previous study on graphene-on-mica (Lui *et al.* 2009). The histograms are well fit by Gaussian distributions (solid lines). Standard deviations (σ) obtained from the Gaussian fits are listed in the figure. The measured surface roughness of mica and graphene on mica (27.3 and 23.4 pm) is similar to a previous study (34.3 and 24.1 pm) (Lui *et al.* 2009). On the other hand, the roughness of the graphite surface is measured to be considerably lower (13.5 pm vs. 22.6 pm), likely due to the differences in the specific settings of AFM. In general we find graphene on water adlayers has slightly lower surface roughness when compared to graphene on mica, which in turn is slightly smoother than the mica surface. These results suggest water molecules may be able to fill in surface defects on the atomic scale. However, as suggested in the previous study (Lui *et al.* 2009), the measured roughness is likely limited by the noise of AFM.

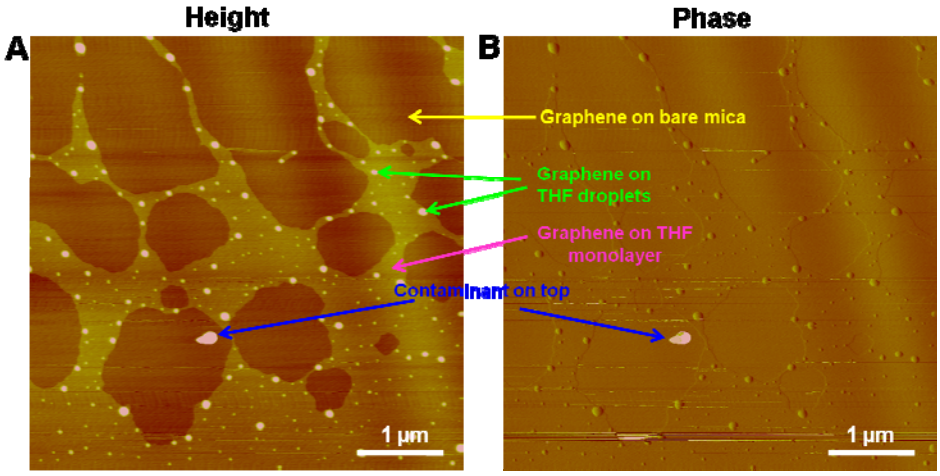

Fig. S7. AFM images of monolayer graphene deposited on a mica surface that was in equilibrium with a tetrahydrofuran (THF) vapor. The mica substrate was first heated in air at 200 °C for 10 min to remove any absorbed moisture, and then transferred into a glove-bag, in which a RH of <2% was maintained. The mica surface was cleaved in the glove-bag, and then exposed to a THF vapor for ~10 s before graphene was deposited. The imaging measurements were done several hours later. (**A**) AFM height image of a single monolayer graphene sheet on this surface. Height scale: 4 nm. (**B**) The corresponding phase image, differentiating a contaminant on top of graphene (blue arrows) from the THF structures under the graphene sheet. Regions identified as graphene on bare mica, graphene on a monolayer of THF, as well as graphene on THF droplets, are indicated.

References for the Supporting Online Material

Garcia, R. and Perez, R. (2002). "Dynamic atomic force microscopy methods." *Surf. Sci. Rep.* **47**, 197.

Lee, C., Li, Q. Y., Kalb, W., Liu, X. Z., Berger, H., Carpick, R. W. and Hone, J. (2010). "Frictional characteristics of atomically thin sheets." *Science* **328**, 76.

Lui, C. H., Liu, L., Mak, K. F., Flynn, G. W. and Heinz, T. F. (2009). "Ultraflat graphene." *Nature* **462**, 339.

Novoselov, K. S., Jiang, D., Schedin, F., Booth, T. J., Khotkevich, V. V., Morozov, S. V. and Geim, A. K. (2005). "Two-dimensional atomic crystals." *Proc. Natl. Acad. Sci. U. S. A.* **102**, 10451.